J. Fluid Mech. (1988), *vol.* 195, *pp.* 161–173
Printed in Great Britain

On the pairing process in an excited plane turbulent mixing layer

By I. WYGNANSKI†‡ AND I. WEISBROT†

†Faculty of Engineering, Tel-Aviv University, Ramat-Aviv, Tel-Aviv 69978, Israel

‡Department of Aerospace and Mechanical Engineering, University of Arizona, Tucson, AZ 85721, USA.

(Received 13 October 1987 and in revised form 19 February 1988)

The flow field in a plane, turbulent mixing layer disturbed by a small oscillating flap was investigated. Three experiments were carried out: one in which the flap oscillated sinusoidally at a single frequency: a second in which the flap oscillated at two frequencies, a fundamental and a subharmonic, but the ensuing motion was dominated by the fundamental perturbation; and a third in which the amplitude of the subharmonic perturbation was increased until a distortion in the mean flow was noticeable. Two velocity components were measured at all phase angles relative to the subharmonic oscillation of the flap at densely spaced intervals. The data were used to map the phase-locked spanwise vorticity component and the phase-locked streakline patterns for the purpose of assessing the relevance of the latter to the understanding of the dynamical process involved.

1. Introduction

Large coherent structures are intrinsic features of all free, turbulent shear flows in general and of the mixing layer in particular. They were discovered by using different techniques of flow visualization, such as shlieren (Crow & Champagne 1971), shadowgraph (Brown & Roshko 1974), or dye injection (Winant & Browand 1974). Whereas photographs using shlieren or shadowgraph techniques are sensitive to the instantaneous gradients in the index of refraction existing at the time of exposure and thus outline the boundaries of the vortical fluid, photographs using dye or smoke represent streaklines. The latter depend on the location of the injector, the amount and initial distribution of the injected material (i.e. whether it marks the entire vortical region of the fluid at the point of injection), and the rate of diffusion between the injected material and the fluids being mixed. Flow visualization had a major impact on our outlook on turbulent shear flows, but it seldom provided the quantitative data needed to understand and control the dynamics of the processes involved. In the case of the mixing layer, concepts like roll-up and pairing became a part of the common jargon, which is often being used without adequate consideration of the implied meanings.

Roll-up implies the folding, rolling, and breakup of a continuous vortex sheet into discrete vortices, while pairing implies a sequential amalgamation of these vortices into larger vortical structures. Ho & Huerre (1984) classify roll-up as an inherently nonlinear effect occurring at a location at which the fundamental frequency attains its maximum amplitude and is accompanied by the generation of a subharmonic frequency. The nonlinear aspect of the roll-up is never quantified but, since the process is identified with flow visualization, one assumes that it stems from a roll-up

of streaklines or species (see, for example, Roberts 1985). Hama (1962) observed that a linear superposition of a weak travelling sine wave on a hyperbolic-tangent velocity profile results in a streakline pattern that rolls up into an array of discrete vortices. This suggests that the inclusion of nonlinear terms is not essential for the prediction of roll-up and the generation of harmonics in the flow may not represent a necessary condition for its occurrence.

Successive amalgamation of pairs of neighbouring vortices marked by dye was visually observed by Winant & Browand (1974), who attributed the divergence of the mixing layer to this process. They argued that the vorticity is continuously being redistributed into larger and larger eddies, whose size doubles at each interaction. The location at which pairing occurs coincides, according to Ho & Huang (1982), with the location at which the subharmonic frequency attains a maximum. Consequently, pairing is intimately associated with the existence of two frequencies in the flow: a fundamental – considered to be the most amplified frequency at the trailing edge of the splitter plate – and a subharmonic, which attains a maximum amplitude farther downstream. Ho & Huang showed that any number of eddies can be made to merge whenever the mixing layer is excited externally by a frequency corresponding to a rational fraction of the dominant frequency at the initiation of mixing. A single vortex amalgamation may require the coexistence of two distinct waves in the flow, while more waves are necessary in order to repeat the process farther downstream. The relationship between vortex amalgamation and the divergence of the mixing layer is not clear. One may observe, from the photographs taken by Brown & Roshko (1974), that the mixing layer diverges in spite of the absence of any visible amalgamations. The digital image analysis of Hernan & Jimenez (1982) concurs with this observation and attributes most of the divergence of the mixing layer to the growth of the large eddies and not to the pairing process.

In order to establish the cause for the divergence of the mixing layer and the role of the subharmonic frequency in this process, one has to first define pairing in terms of measurable quantities. For this purpose, the mixing layer was excited at two synchronized frequencies, $F_f = 36$ Hz and $F_s = 18$ Hz, which will be referred to in the text as the fundamental and the subharmonic, although F_f is not the most amplified frequency at the trailing edge of the splitter plate. The experiments were conducted in a mixing-layer facility described by Oster & Wygnanski (1982); the velocity of the faster stream was 8 m/s, while the speed of the slower stream was 4.8 m/s. Thus, the average convection speed of the large eddies is $U_c = 0.5(U_1+U_2) = 6.4$ m/s and the ratio of velocities described by the parameter $R = (U_2-U_1)/(U_2+U_1)$ is 0.25. Two components of velocity were measured at 80 X-stations separated by 20 mm in the direction of streaming, corresponding approximately to one-tenth of the wavelength of the fundamental frequency. The measurements were taken with a rake containing 7 X-wire probes which was traversed across the flow. The velocities measured at each point were sampled at 2.048 kHz, together with the two sinusoidal voltages activating the flap, for a total duration exceeding 1000 cycles of the fundamental frequency. The input voltages were used to obtain a phase reference for averaging the data. The phase-locked data were used to compute the coherent velocity fluctuations, as well as the coherent spanwise component of vorticity, without the need to resort to Taylor's hypothesis. The high spatial and temporal resolution of the data was required for the calculations of particle paths and streaklines used to simulate flow visualization. Identical data, therefore, were used to describe the dynamics of the flow in a laboratory coordinate system and to describe the paths of particles in the

disturbed flow field. Consequently, any pattern observed in the Lagrangian frame of reference has a precise experimental counterpart in an Eulerian system. The purpose for this exercise was to define the implied relationships between flow visualization and measurement in the disturbed, two-dimensional mixing layer.

2. Results

2.1. *The mixing layer excited by a single travelling wave*

The experimental methods were first tested in a mixing layer excited by a single travelling wavetrain described by Weisbrot & Wygnanski (1988). A visual resemblance was established between streaklines calculated from the phase-locked velocity measurements and photographs obtained by stroboscopic illumination synchronized with the flap motion and using smoke as a means of flow visualization. The photographs taken represented either a single realization or an ensemble average of many events, depending on the time of exposure; a visual comparison of such photographs did not reveal any significant large-scale feature that was not observed in the ensemble average.

A pattern of 7 streaklines originating from hypothetical sources located at $\bar{X} = RF_f X/U_c = 0.28$ downstream of the splitter plate and displaced by a distance of $\Delta\bar{Y} = \Delta Y F_f/U_c = 0.011$ around the centreline of the mixing layer was calculated (for the particular choice of the dimensionless group, see Oster & Wygnanski 1982). Although data are available for the entire distance between $\bar{X} = 0.28$ and $\bar{X} = 2.5$ from the trailing edge of the splitter plate, the pattern shown in figure 1(*a*) covers only one-half of this distance since, in this interval, the vortex sheet rolls up into the characteristic row of discrete lumps.

One may observe that particles emanating from the high-speed side of the mixing layer are convected downstream faster than particles emanating from the low-speed side, causing an accumulation of particles at the crest of the wave and resulting in the roll-up of the streaklines. The streamwise location at which roll-up is observed depends on the phase angle between the streakline pattern and the flap; the roll-up process is centred around $\bar{X} = 0.625$. The effect of the presence of other modes (or frequencies) generated by nonlinear interactions on the roll-up process may be estimated by filtering out all the frequencies with the exception of the fundamental from the time series, representing phase-locked ensemble-averaged velocities measured throughout the flow field, and recalculating the streakline pattern. The results of these calculations are shown in figure 1(*b*). Although the roll-up process is impeded somewhat by the absence of the nonlinear terms, it is not eliminated. The vortex sheet keeps rolling up into lumps of concentrated vorticity and keeps stretching and thinning in between. The leading nonlinear term in this experiment is the harmonic constituent of the spectrum, which contributes as much as 30% to the average (integrated across the shear layer) amplitude of the phase-locked velocity signal at $\bar{X} \approx 0.7$ (corresponding to $X = 500$ mm in figure 8(*c*) of Weisbrot & Wygnanski 1988).

The corresponding filtered contours of the spanwise component of vorticity are plotted on an expanded $\bar{X}$-scale in figure 2(*a*). The various harmonics have some effect on the intensity of the measured vorticity (see figure 17 of Weisbrot & Wygnanski 1988) but not on its distribution inside the shear layer. Within the resolution of the experiment, the spanwise component of the coherent vorticity becomes concentrated in discrete lumps having dimensions that are commensurate with the dimensions of the eddies represented by the concentration of particles. It is interesting to note that

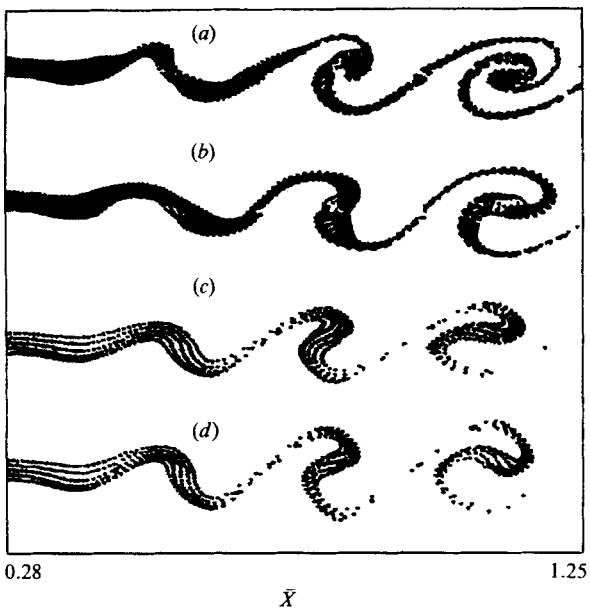

FIGURE 1. Phase-locked streaklines in a mixing layer excited by a single frequency: (a) unfiltered, (b) filtered, (c) calculated initial amplitude 3%, (d) 5%.

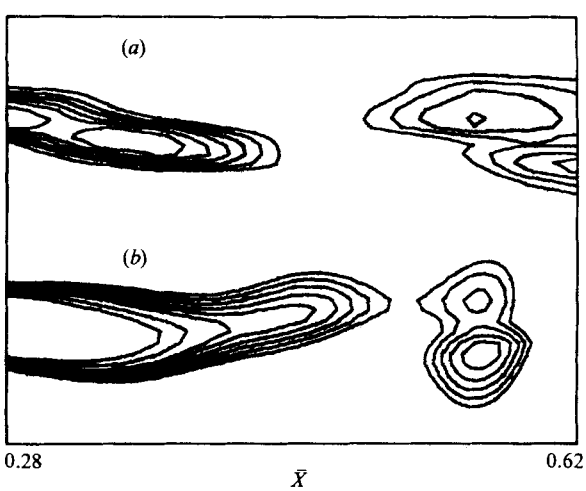

FIGURE 2. Vorticity distribution corresponding to streaklines shown in figures 1(b) and 1(d).

vorticity is not uniformly distributed over a single wavelength (or period) of the perturbed shear layer, even far upstream of the location at which roll-up occurs. By observing the vorticity contours generated at various time delays or phase angles relative to the flap, one can follow the process by which the concentrated vorticity on the high-speed side of the mixing layer catches up with the vorticity concentration on the low-speed side. At an X-location corresponding to the roll-up of the particles, the two concentrations of vorticity become displaced in the transverse direction only. Farther downstream (figure 16 of Weisbrot & Wygnanski 1988), the boundary between the two concentrations of vorticity disappears and one is left with a single vortical structure, which is convected downstream. By overlaying the vorticity

contours on the streakline pattern, one may notice that, at larger downstream distances, there is some discrepancy in the overall dimension of the two patterns. This discrepancy might be partly reduced by increasing the number of streaklines calculated, as well as lowering the initial contour level plotted in figure 2. Nevertheless, more particles are always concentrated at the trailing (upstream) part of the vortex, while the leading (downstream) portion of the vortical structure spans the gap between the lumpy concentration of particles and the thin braid preceding it. Thus, a lack of particles on the high-velocity side of the braid does not necessarily imply that the flow is entirely irrotational.

It had been shown by Gaster, Kit & Wygnanski (1985) that linear stability theory, applied to a prescribed mean flow field, predicts quite well the transverse distribution of disturbances produced by a travelling wave. It is interesting, therefore, to compare the observations cited above with the linear model, in spite of the fact that the latter does not correctly predict the amplification in the direction of streaming. A streakline pattern was calculated using a simple inviscid model for the perturbation which was superimposed on a divergent mean velocity profile identical to the one described in equation (5.2) of Gaster *et al.* The divergence angle $\mathrm{d}x/\mathrm{d}\theta$ applicable to this experiment was 37.7, and the value of X_0 was 83 mm. The differences stem from the larger amplitude of the imposed excitation. Since the decaying modes could not have been calculated using the inviscid model, one had to assume that the perturbation retained its amplitude and shape downstream of the neutral point. One could easily modify this constraint, but it did not seem to warrant the additional computational effort. The results of these calculations are plotted in figures 1(*c*) and 1(*d*) for initial dimensionless amplitudes of the perturbations (at $\bar{X} = 0.28$) of 3% and 5%. Although the detailed comparison between experiment and computation reveals some minor differences, it is evident that the linear model captures the main features of the roll-up process. Hama (1962), who computed the streaklines resulting from a linear superposition of a neutral sinusoidal disturbance on a parallel shear layer, concluded that the complex streakline pattern observed is caused by particles being trapped within the recirculating ('cat's eye'-shaped) streamlines which are computed in a reference frame moving at U_c. This also is the case in the present investigation.

The distribution of vorticity in the perturbed mixing layer was also computed by using the inviscid model, and the results are shown in contour form in figure 2(*b*). Once again, the main features of vorticity redistribution are captured by the simple model, in spite of the quantitative differences attributed, in part, to the inadequate prediction of the amplification rate in the direction of streaming (see figure 7 of Weisbrot & Wygnanski 1988). The most important feature shown in figure 2(*b*), which is also confirmed by experiment, is the roll-up of vorticity from an undulating sheet to a lumpy structure. This roll-up occurs whenever the imposed perturbation becomes neutrally stable as a result of the divergence of the mean flow. Somewhat similar vorticity contours were computed by Michalke (1964) for a temporally evolving perturbation in a parallel shear layer. Whenever the perturbation is strongly amplified, the vorticity is concentrated in two cores which are displaced in time and in the transverse direction; at the neutral point, however, the vorticity is reorganized into a single core spanning the entire width of the mixing layer (see figure 10 in Michalke 1964 and figures 38 and 39 of Oster & Wygnanski 1982).

Browand & Weidman (1976) drew vorticity contour maps based on conditionally sampled measurements in an unexcited mixing layer. The conditional-sampling algorithm was supported by flow visualization in which dye was injected into the

boundary layer generated on the splitter plate. The contours shown in figure 6 of their manuscript are very similar to the contours shown here in figure 2, provided one keeps in mind that the location of the high-velocity stream is inverted in the two sets of figures. Browand & Weidman refer to the lumpy vorticity distribution showing a single core in the centre as the one generated during the final stages of pairing. They define an intermediate stage of pairing as the one being similar to the distribution shown on the left-hand side of figure 2 (i.e. for $\bar{X} \leqslant 0.5$).

One may adopt the view that the pairing process and the reorganization of vorticity, resulting from the divergence of the mean flow during the time in which a wavy disturbance is being amplified, are one and the same. Pairing is completed when the primary disturbance becomes neutrally stable to its local environment. Browand & Weidman (1976) observed that the Reynolds stress generated during the intermediate stages of the pairing is twice as high as the Reynolds stress observed at the end of this process. This can be explained by the fact that the Reynolds stress produced by large coherent structures vanishes when the pairing process is complete (see figures 9 and 10 of Weisbrot & Wygnanski 1988). The mean flow responds to the reduction in the Reynolds stress by a concomitant reduction in the angle of divergence which, in an externally excited flow, can even become negative. The new interpretation which lumps pairing and roll-up together as representing the same process has to reconcile numerous difficulties, such as: (i) The streaklines observed in the present experiment show no sign of amalgamation, while the lumps of dyed fluid in the experiments of Browand & Weidman (1976) merge in the process. (ii) The amplitude of the subharmonic frequency in the present experiments was negligible, yet the subharmonic frequency is reported to control vortex pairing (Ho & Huerre 1984). One may ask, therefore if the presence of a subharmonic is a necessary condition for the pairing process. These questions will be addressed in the next section.

2.2. *The mixing layer excited by two waves – a fundamental and a subharmonic*

The mixing layer in this experiment was excited by the two synchronized perturbations described in the introductory section. The initial amplitude of the fundamental frequency measured at $X \approx 160$ mm downstream of the splitter plate and shown in figure 3 was approximately twice as high as that of the subharmonic, while the harmonic frequency indicating the initial degree of nonlinearity was at least one order of magnitude lower than the fundamental. The dimensionless parameter $RF_f X/U_c$ is no longer useful in this case because the evolution of the flow is affected by the *two excited wavetrains*, their amplitudes, and the emerging nonlinear interactions. The fundamental frequency became saturated at $X \approx 700$ mm, while the rate of amplification of the subharmonic increased at that location. Between $X = 700$ mm and $X = 1000$ mm from the splitter plate, the fundamental wave and its harmonic retained their intensity while the integrated amplitude of the subharmonic doubled. At $X > 1000$ mm, the fundamental and its harmonic started to decay while the rate of amplification of the subharmonic with X increased further and, at $X = 1160$ mm, the amplitude of the subharmonic surpassed the amplitude of the fundamental. The width of the shear layer θ, which was fairly constant between $X \approx 700$ mm and $X \approx 1100$ mm, resumed its lateral growth also at $X = 1160$ mm. The changes in the rate of amplification of F_s suggest that the subharmonic frequency derives some of its growth from a nonlinear interaction with the fundamental; perhaps it even resonates with the fundamental in a manner described by Kelly (1967) and observed experimentally in a circular mixing layer by Cohen & Wygnanski (1987).

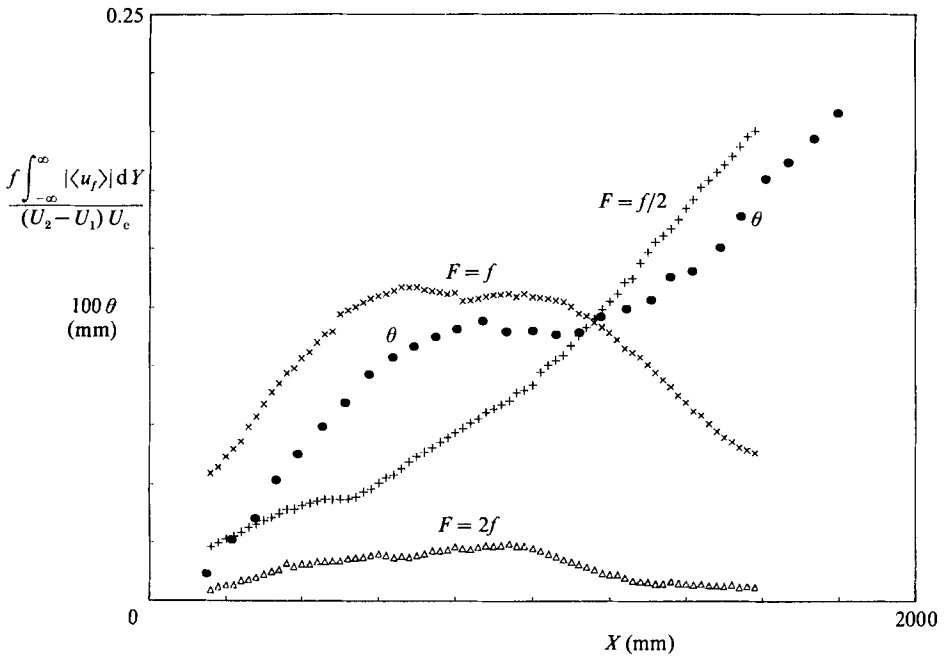

FIGURE 3. The amplitudes of $\langle u\rangle_f$, $\langle u\rangle_{f/2}$, and $\langle u\rangle_{2f}$ integrated across the flow at various X-locations and the variation of the momentum thickness θ with X.

Two patterns of streaklines, one originating at the first X-station at which measurements were made (i.e. at $X = 160$ mm) and the other originating at the X-station at which the fundamental frequency attained its maximum amplitude (i.e. at $X = 600$ mm), were calculated. The motion of the flap was subdivided into five equal segments; thus, the patterns shown in figure 4 correspond to different phases of the excitation. One can clearly discern two lumps of tagged fluid undergoing amalgamation in figure 4*a*. The process starts at $X \approx 400$, where one lump of fluid is displaced vertically upwards (towards the high-speed flow) and proceeds to overtake the lower lump while both lumps are convected downstream. The two lumps are being strained while rotating around each other in a manner reminiscent of the observations of Winant & Browand (1974) and Browand & Weidman (1976). The amalgamation is almost complete at $X = 1000$ mm.

The flow field that gave rise to the streakline pattern shown in figure 4(*b*) was *identical in all its detail* to the flow field responsible for the pattern shown in figure 4(*a*): only the location of the source of the imaginary dye or smoke injector was changed. Nevertheless, one cannot observe a pairing interaction in figure 4(*b*) that is as clearly discernible as the one in figure 4(*a*). Cimballa (1984), who examined the streaklines generated by smoke injected into a wake of a circular cylinder, pointed out that the pattern that he photographed depended on the location of his smoke generator. Both observations suggest that flow visualization based on streaklines has to be treated with caution.

Since the eddies undergoing pairing in figure 4(*a*) are sandwiched between other eddies that do not pair, one can assess the size of the ensuing vortical structure, and the concentration of vorticity within it, relative to its unpaired neighbours both upstream and downstream. The vorticity contours shown in figure 5 during a roll-up or during a pairing interaction are almost identical, regardless of the differences in

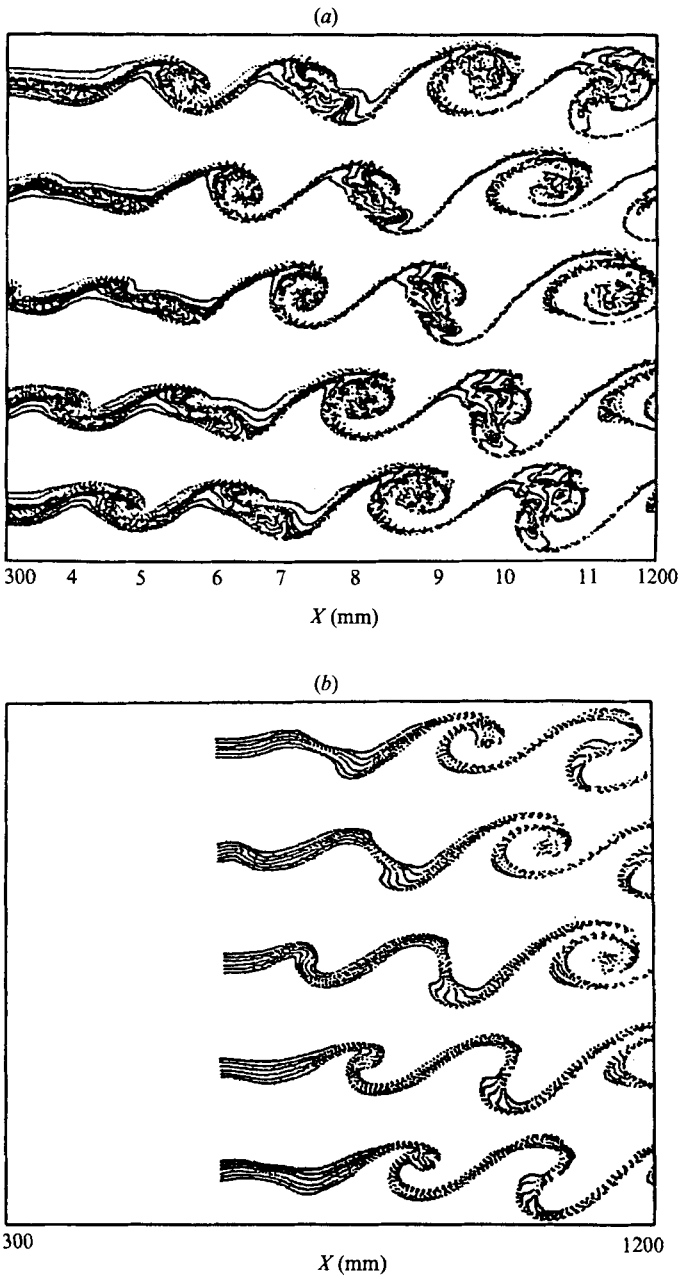

FIGURE 4. Streaklines in a mixing layer excited by a strong fundamental and a weak subharmonic: (a) particles tagged at $X = 160$ mm, (b) particles tagged at $X = 600$ mm.

the streakline patterns, and resemble the vorticity distribution discussed in the previous section. *Therefore, both roll-up and pairing appear to have the same significance when interpreted in terms of vorticity.* At both instances, the reorganization of vorticity corresponds to the X-location at which the amplitude of the dominant perturbation became saturated or, in the context of the linear stability theory, the flow became neutrally stable to the predominant perturbation. Since roll-up and pairing might be one and the same, the overall response of the mixing layer to either

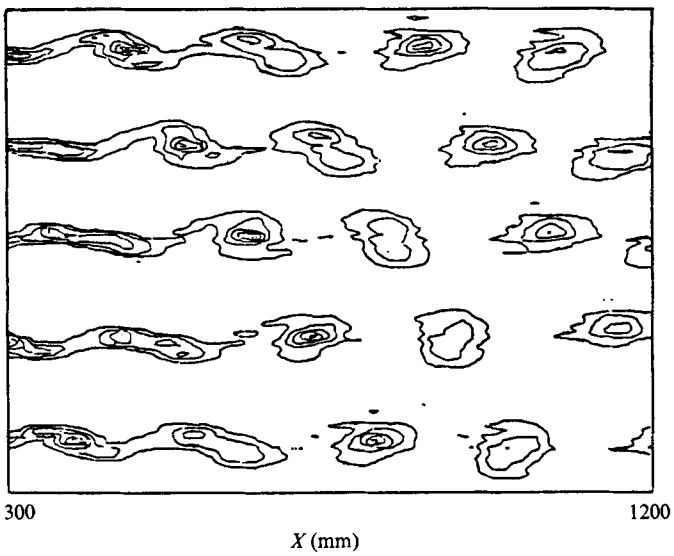

FIGURE 5. Vorticity distribution corresponding to streaklines shown in figure 4.

should also be identical. This observation has already been made by Ho & Huerre (1984), although it was not recognized as such. The only difference between the data presented by Ho & Huerre in their figure 19 and in figure 3 stems from the fact that the eddies shown in figure 19 went through the roll-up process twice – once corresponding to F_f and then corresponding to F_s. It is interesting to note (figure 5) that the vorticity concentration corresponding to the eddies undergoing 'pairing' is weaker than it is for the simply rolled eddies; this is attributed in part to a nonlinear process which will be discussed later.

The importance of the subharmonic frequency (F_s) in the amalgamation process observed in figure 4(*a*) is considered by decomposing the signal into its Fourier constituents and reconstructing the streakline pattern as discussed in the previous section. Spectral analysis reveals that, in addition to F_f and F_s, which were externally introduced by the motion of the flap, two additional frequencies are present in the flow: F_h, which is generated by the finite amplitude of the fundamental, and $F_{\text{sum}} = F_f + F_s$, which is generated by the nonlinear interaction of the fundamental and the subharmonic or by a secondary interaction between F_h and F_s. Taking one frequency at a time and superimposing it on the mean velocity field results in a regular array of eddies which do not coalesce (figure 6); in fact, F_s by itself does not even roll up within the distance considered. The streakline pattern constructed by the superposition of F_{sum} on the mean velocity profile is somewhat distorted when compared with the pattern based on F_f or F_h, presumably because F_{sum} is generated by a combination of nonlinear interactions.

By linearly superimposing either two or three of the dominant frequencies on the mean velocity profile and recomputing the streakline patterns, one obtains the variety shown in figure 7. It is obvious that the combination of the fundamental with either the subharmonic or the harmonic, or both together, does not result in the apparent amalgamation of eddies shown in figure 4(*a*) and replotted for convenience at the top of figure 7. It is therefore the fundamental, in conjunction with F_{sum}, which is responsible for the 'pairing' effect observed at $X = 650$ mm in figure 7. One should not infer that the subharmonic will not cause the amalgamation of streaklines farther

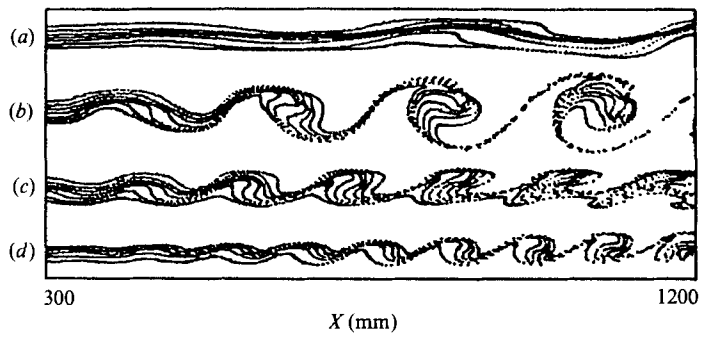

FIGURE 6. Streaklines corresponding to data shown in figure 4 which were generated by filtering and retaining only one frequency as marked: (a) F_s, (b) F_f, (c) F_{sum}, (d) F_h.

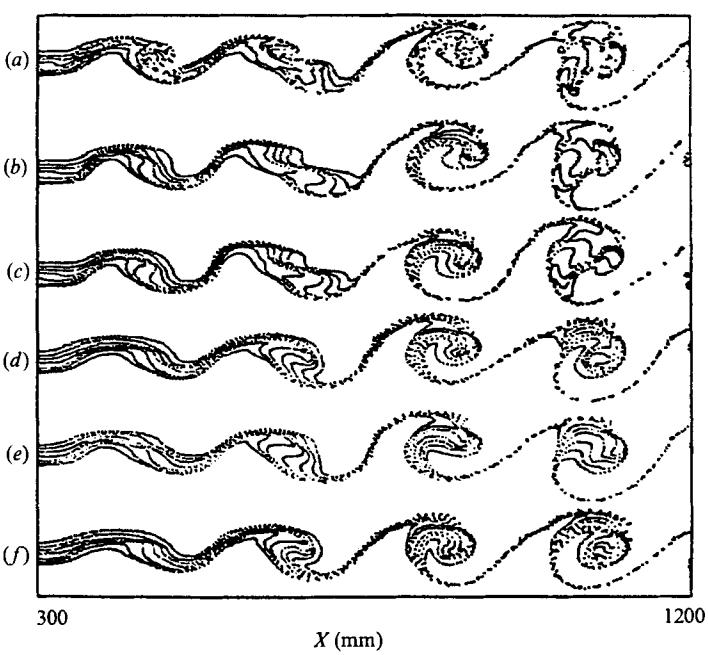

FIGURE 7. Streakline patterns representing a combination of frequencies: (a) same as in figure 4(a), (b) $F_s+F_f+F_{\text{sum}}$, (c) F_f+F_{sum}, (d) $F_s+F_f+F_h$, (e) F_s+F_f, (f) F_f+F_h.

downstream (the beginnings of this process are, in fact, detected near the end of the test section); it is simply preceded by F_{sum}, which rolled up somewhat upstream of the fundamental (figures 6*b*, *c*). The perturbation associated with F_{sum} is out of phase with the fundamental every two wavelengths of F_f, which gives rise to the apparent pairing interaction and the concomitant reduction in the intensity of the vorticity concentration observed in figure 5. One may also note that, upon the completion of roll-up, the vorticity contours appear to be almost circular. During either amplification or decay, these contours have elongated, elliptical shapes in which the inclination of the major axis changes by $\frac{1}{2}\pi$ when they pass from a state of growth to a state of decay. The generation of Reynolds stress and the transfer of momentum between the mean motion and the large structures depend on the tilt of these eddies, as observed by Browand & Ho (1983).

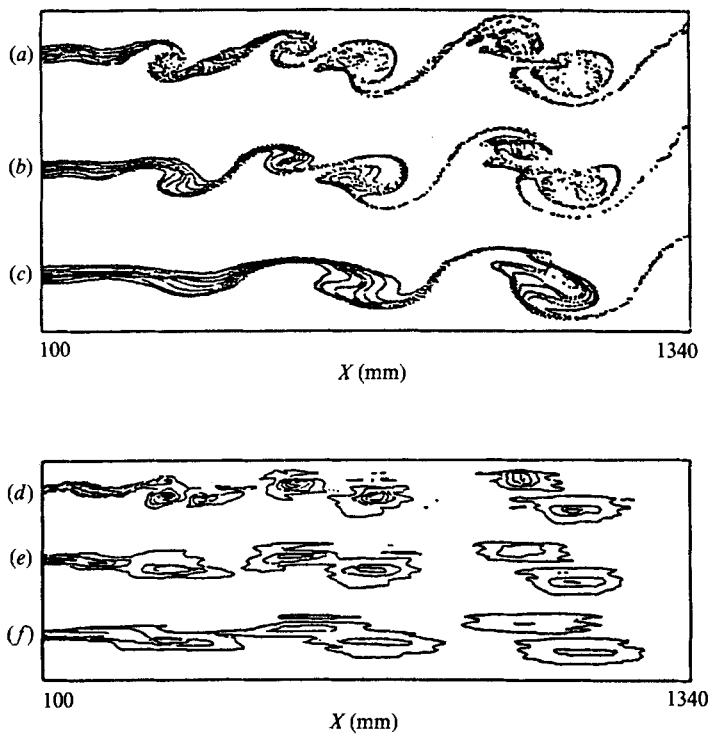

FIGURE 8. Streakline and vorticity patterns for 'pairing' resulting from an interaction of a fundamental and a subharmonic: (*a*, *d*) unfiltered, (*b*, *e*) F_s+F_f, (*c*, *f*) F_s.

In order to show that a 'pairing interaction' can occur on the scale of the subharmonic wave, the initial excitation level of the subharmonic frequency was increased. A vigorous 'pairing' was observed in the streakline pattern based on the unfiltered, phase-locked velocities shown in figure 8(*a*). When all frequencies other than F_s and F_f were removed from the time series, the pairing interaction remained virtually unchanged (figure 8*b*). The pairing process, however, entirely disappeared from the streakline pattern by the removal of F_f (figure 8*c*), showing an impending roll-up of the subharmonic instead. The accompanying vorticity contours, shown in figure 8(*d–f*), were not restructured by the removal of all frequencies other than F_f and F_s nor were they reorganized by the removal of the fundamental. The concentration of vorticity within the large eddies was simply reduced somewhat by the selective removal of all but the subharmonic frequency, as indicated by the number of contours plotted in the respective figures. Since the disappearance of 'pairing' from the streakline pattern (figure 8*c*) was not accompanied by a redistribution of vorticity (figures 8*e*, *f*), the former effect cannot be significant to the dynamics of the flow. On the other hand, the impending reorganization of vorticity at the subharmonic frequency is similar to the process discussed in conjunction with the data presented in figure 2, implying that such reorganization signifies a switch from an amplification stage to a decay stage of a given disturbance.

3. Conclusions

A simple, model flow field generated by a linear superposition of sinusoidal disturbances on a two-dimensional shear layer results in a complex pattern of streaklines which roll, amalgamate, or even tear one another (see Wygnanski & Petersen 1985), figure 14). One should not rely, therefore, on flow visualization alone for the purpose of formulating concepts pertaining to the dynamics of the flow. It is obvious that simple dynamical systems may produce complex particle trajectories. One may attribute both 'pairing' and 'roll-up' to a redistribution of vorticity resulting from a neutral amplification of the most energetic wavy disturbance in the flow. The sole nonlinearity needed to predict this process, at least qualitatively, is implied by the divergence of the mean motion which would not have occurred were it not for the finite amplitudes of the predominant disturbances. A shear layer which is excited externally by a single wavetrain at a frequency f will generate a large harmonic content (at a frequency $2f$) before the occurrence of 'roll-up', but the generation of a subharmonic frequency is not a prerequisite for this process. The experimental results discussed (see, also, Weisbrot & Wygnanski 1988) indicate that weakly nonlinear models based on stability theory may predict quite well the interaction between the mean flow and the large-scale structures in two dimensions.

This study was supported in part by AFOSR Grant 86-0323 and by ONR Contract N 00014-85-K-0412.

REFERENCES

BROWAND, F. K. & HO, C. M. 1983 The mixing layer: an example of quasi two-dimensional turbulence. *J. Méc. Théor. Appl. Numero Special*, pp. 99–120.

BROWAND, F. K. & WEIDMAN, P. D. 1976 Large scales in the developing mixing layer. *J. Fluid Mech.* **76**, 127–144.

BROWN, G. L. & ROSHKO, A. 1974 On density effects and large structure in turbulent mixing layers. *J. Fluid Mech.* **64**, 775–816.

CIMBALLA, J. M. 1984 Large structure in the far wakes of two-dimensional bluff bodies. Ph.D. thesis, California Institute of Technology.

COHEN, J. & WYGNANSKI, I. 1987 The evolution of instabilities in the axisymmetric jet. Part 2. Flow resulting from the interaction of two waves. *J. Fluid Mech.* **176**, 221–235.

CROW, S. C. & CHAMPAGNE, F. H. 1971 Orderly structure in jet turbulence. *J. Fluid Mech.* **48**, 547–591.

GASTER, M., KIT, E. & WYGNANSKI, I. 1985 Large-scale structures in a forced turbulent mixing layer. *J. Fluid Mech.* **150**, 23–39.

HAMA, F. R. 1962 Streaklines in a perturbed shear flow. *Phys. Fluids* **5**, 644–650.

HERNAN, M. A. & JIMENEZ, J. 1982 Computer analysis of a high-speed film of the plane turbulent mixing layer. *J. Fluid Mech.* **119**, 323–345.

HO, C. M. & HUANG, L. S. 1982 Subharmonics and vortex merging in mixing layers. *J. Fluid Mech.* **119**, 443–473.

HO, C. M. & HUERRE, P. 1984 Perturbed free shear layers. *Ann. Rev. Fluid Mech.* **16**, 365–424.

KELLY, R. E. 1967 On the stability of an inviscid shear layer which is periodic in space and time. *J. Fluid Mech.* **27**, 657–689.

MICHALKE, A. 1964 On the inviscid instability of the hyperbolic tangent velocity profile. *J. Fluid Mech.* **19**, 543–556.

OSTER, D. & WYGNANSKI, I. 1982 The forced mixing layer between parallel streams. *J. Fluid Mech.* **123**, 91–130.

ROBERTS, F. A. 1985 Effects of periodic disturbance on the structure and mixing in turbulent shear layers and wakes. Ph.D. thesis, California Institute of Technology.

WEISBROT, I. & WYGNANSKI, I. 1988 On coherent structures in a highly excited turbulent mixing layer. *J. Fluid Mech.* **195**, 137–159.

WINANT, C. D. & BROWAND, F. K. 1974 Vortex pairing, the mechanism of turbulent mixing-layer growth at moderate Reynolds numbers. *J. Fluid Mech.* **63**, 237–255.

WYGNANSKI, I. & PETERSEN, R. A. 1985 Coherent motion in excited free shear flow. *AIAA Paper* 85-0539.